





BRIEF DEFINITIVE REPORT

4-1BB costimulation induces T cell mitochondrial function and biogenesis enabling cancer immunotherapeutic responses

Ashley V. Menk¹, Nicole E. Scharping^{1,2} , Dayana B. Rivadeneira^{1,2}, Michael J. Calderon³, McLane J. Watson^{1,2} , Deanna Dunstane¹, Simon C. Watkins^{2,3} , and Greg M. Delgoffe^{1,2} 

Despite remarkable responses to cancer immunotherapy in a subset of patients, many patients remain resistant to these therapies. The tumor microenvironment can impose metabolic restrictions on T cell function, creating a resistance mechanism to immunotherapy. We have previously shown tumor-infiltrating T cells succumb to progressive loss of metabolic sufficiency, characterized by repression of mitochondrial activity that cannot be rescued by PD-1 blockade. 4-1BB, a costimulatory molecule highly expressed on exhausted T cells, has been shown to influence metabolic function. We hypothesized that 4-1BB signaling might provide metabolic support to tumor-infiltrating T cells. 4-1BB costimulation of CD8⁺ T cells results in enhanced mitochondrial capacity (suggestive of fusion) and engages PGC1 α -mediated pathways via activation of p38-MAPK. 4-1BB treatment of mice improves metabolic sufficiency in endogenous and adoptive therapeutic CD8⁺ T cells. 4-1BB stimulation combined with PD-1 blockade results in robust antitumor immunity. Sequenced studies revealed the metabolic support afforded by 4-1BB agonism need not be continuous and that a short course of anti-4-1BB pretreatment was sufficient to provide a synergistic response. Our studies highlight metabolic reprogramming as the dominant effect of 4-1BB therapy and suggest that combinatorial strategies using 4-1BB agonism may help overcome the immunosuppressive metabolic landscape of the tumor microenvironment.

Introduction

For many advanced cancers, immunotherapy has become an attractive and viable option for treatment (Callahan et al., 2016). Probably most well-known is the monoclonal antibody-mediated blockade of programmed death 1 (PD-1), a coinhibitory “check-point” molecule expressed on the surface of activated tumor-infiltrating T cells, or its ligand, PD-L1. This blockade allows for TCR and CD28-mediated signaling in the tumor microenvironment, resulting in increased effector function and antitumor immunity (Hui et al., 2017; Kamphorst et al., 2017). Although those patients that respond to PD-1 blockade can achieve long-term durable responses, in most indications the proportion of patients is still low (10–30%; Callahan et al., 2016). This is in spite of the fact that PD-1 acts as a general inhibitory factor in T cell activation, and blocking this signal should lead to increased T cell activation. Thus, understanding how T cells are regulated in the tumor microenvironment is of major importance because any inhibitory pathways represent potential resistance mechanisms to PD-1-blockade immunotherapy.

Although blockade of inhibitory molecules represents one successful strategy to invigorating the antitumor immune response, another approach involves the exogenous stimulation of additional costimulatory signals in the tumor microenvironment. One of these approaches involves the costimulatory molecule 4-1BB/CD137. 4-1BB is a member of the TNFR family of costimulatory receptors and is expressed on activated CD4 and CD8 T cells (Sanchez-Paulete et al., 2016). 4-1BB has been previously shown to act as a potent costimulator of T cells, promoting T cell proliferation and expansion as well as the acquisition of a more memory-like phenotype (Willoughby et al., 2014). However, the ligand for 4-1BB is expressed predominantly by proinflammatory antigen-presenting cells, suggesting that in the highly immunosuppressive tumor microenvironment there is little source of 4-1BB stimulation. Like CD28, 4-1BB can be ligated by using soluble stimulatory monoclonal antibodies both in vitro and in vivo, and as such researchers have suggested use of 4-1BB as a means to promote antitumor immunity (Sanchez-Paulete

¹Tumor Microenvironment Center, UPMC Hillman Cancer Center, University of Pittsburgh, Pittsburgh, PA; ²Department of Immunology, University of Pittsburgh, Pittsburgh, PA; ³Department of Cell Biology, University of Pittsburgh, Pittsburgh, PA.

Correspondence to Greg M. Delgoffe: gdelgoffe@pitt.edu.

© 2018 Menk et al. This article is distributed under the terms of an Attribution–Noncommercial–Share Alike–No Mirror Sites license for the first six months after the publication date (see <http://www.rupress.org/terms/>). After six months it is available under a Creative Commons License (Attribution–Noncommercial–Share Alike 4.0 International license, as described at <https://creativecommons.org/licenses/by-nc-sa/4.0/>).

et al., 2016). However, a wealth of preclinical data suggests that 4-1BB has little activity as a monotherapy, save in very immunogenic tumor models (Sanchez-Paulete et al., 2016). Clinical trials of 4-1BB monotherapy, too, have not yielded substantial or durable responses and have been hampered by dose-limiting toxicities (Segal et al., 2017). Combinations of immunotherapies such as vaccination, adoptive T cell transfer, and coinhibitory checkpoint blockade with 4-1BB stimulation have suggested a synergistic beneficial effect on antitumor immunity (Sanchez-Paulete et al., 2016). However, the mechanisms by which 4-1BB may potentiate immunotherapeutic response remain unclear.

It has recently been appreciated that the metabolic landscape of the tumor microenvironment may represent an additional resistance mechanism to immunotherapy (Delgoffe, 2016). T cell effector responses are energetically demanding, and T cells undergo substantial metabolic reprogramming during activation, effector phase, and transition to memory to support cellular functions. Tumor cell metabolic deregulation creates an environment characterized by hypoxia, acidosis, and low levels of nutrient sources such as glucose, glutamine, and arginine, thus further limiting T cell function by restricting ultimate cellular function (Scharping and Delgoffe, 2016). Thus, even if a strong immunotherapy such as PD-1 blockade allows for T cell activation and initiation of effector function, T cells may be unable to generate the bioenergetic intermediates necessary to carry out that function.

We have previously shown that T cells infiltrate the tumor microenvironment at a metabolic disadvantage, characterized by repressed glucose uptake and mitochondrial sufficiency, in a manner that was independent of PD-1 blockade or regulatory T cell suppression (Scharping et al., 2016). Chronic activation, in part, represses the activity of a transcriptional coactivator PGC1 α , a transcriptional coactivator that coordinates mitochondrial function and biogenesis (Fernandez-Marcos and Auwerx, 2011). Retrovirally reprogramming tumor-specific cells with PGC1 α resulted in increased antitumor immunity. However, this adoptive T cell therapy approach is both laborious and reliant on several known (and restrictive) experimental variables, including T cell specificity, antigen expression in the tumor microenvironment, and population of initiating cells that was metabolically competent. We thus wondered whether other modulatory interventions might be exploited for metabolic support.

The signaling of 4-1BB, a T cell-bound costimulatory target with much clinical interest, has previously been associated with metabolic reprogramming (Choi et al., 2017), and recent studies using the 4-1BB-signaling domain in chimeric antigen receptor T cells suggest that 4-1BB may act to promote mitochondrial biogenesis and improve metabolism (Long et al., 2015; Kawalekar et al., 2016). T cells go through a variety of metabolic changes during activation, including the up-regulation of glucose uptake (Rathmell et al., 2003; Jacobs et al., 2008) and processing machinery (Gubser et al., 2013) that support aerobic glycolysis, important for cytokine synthesis and epigenetic reprogramming (Chang et al., 2013; Peng et al., 2016). T cells also dramatically remodel their mitochondrial metabolism and, especially during the transition to memory, engage in mitochondrial biogenesis and fusion that support a heightened respiratory capacity, becoming

energetically primed for reactivation (van der Windt et al., 2013; Buck et al., 2016). Indeed, in all cells, mitochondrial capacity is linked to cellular longevity and avoidance of senescence (Ferris et al., 2016). In other words, manipulation of metabolism to promote/enhance mitochondrial function may improve the longevity and memory capacity of T cells, resulting in enhanced anti-tumor potential.

Thus, we sought to determine, both in vitro and in vivo, the metabolic consequences of 4-1BB ligation. We found that 4-1BB costimulation results in activated T cells with superior metabolic capacity. 4-1BB activation, through stimulation of p38-MAPK, results in PGC1 α -dependent mitochondrial fusion and biogenesis. This substantially increased T cell respiratory capacity, a measure of mitochondrial reserve, that could be used upon full T cell activation mediated by CD28 signaling. 4-1BB treatment of WT mice resulted in substantial increases in T cell metabolic capacity in vivo, which promoted a phenotype of intratumoral metabolic sufficiency that enabled responses to adoptive cell and PD-1 blockade-mediated therapy in murine tumors. Further, we found that 4-1BB pretreatment was sufficient to provide metabolic support for a full anti-PD-1 response, suggesting 4-1BB agonists can be sequenced with coinhibitory blockade to increase the penetrance of cancer immunotherapy.

Results and discussion

4-1BB costimulation results in increased mitochondrial function

Costimulation has long been associated with metabolic reprogramming; CD28 ligation, for instance, increases glucose uptake (Jacobs et al., 2008), up-regulation of metabolic machinery (Zheng et al., 2009), and mitochondrial complexity (Klein Geltink et al., 2017), which are important for the avoidance of T cell dysfunctional states such as anergy. Likewise, T cell costimulation is thought to be diminished or missing in intratumoral responses, thus representing an attractive modality to improve both T cell immunological and metabolic responses (Zang and Allison, 2007). In the tumor microenvironment, high-affinity T cells subject to chronic stimulation become exhausted in a stepwise manner that correlates to expression of coinhibitory molecules such as PD-1 and Tim-3 (Wherry and Kurachi, 2015), with the most exhausted T cells likely being tumor-specific and also metabolically repressed. We thus first asked which costimulatory molecules would be present on the cell surface and thus available for optimal stimulation, along the spectrum of tumor-induced T cell exhaustion (PD-1^{lo}, PD-1^{mid}, PD-1^{hi}, and PD-1^{hi}Tim-3⁺), using CD8⁺ T cells infiltrating B16-melanoma tumors. Other coinhibitory molecules associated with exhaustion, such as LAG-3, track with this progression (Fig. S1, A and B). Our analysis showed intratumoral T cells display two patterns of costimulatory molecule expression, with molecules such as CD28, ICOS, and OX40 being repressed or unchanged after the PD-1^{mid} (likely newly activated T cell) stage (Fig. S1 C). However, the TNFR family costimulatory molecule 4-1BB (CD137) was highly up-regulated on terminally exhausted T cells, consistent with previous data (Williams et al., 2017), suggesting that this costimulatory pathway may be ideal for the reinvigoration of the highly tumor-specific, yet exhausted, T cell subset (Fig. S1 D).

To explore the metabolic contribution of this pathway, we first sought to dissect the contribution of 4-1BB to T cell expansion *in vitro*. We activated murine CD8⁺ T cells with plate-bound anti-CD3 in the presence of soluble agonistic antibodies against CD28, 4-1BB, or both. Although CD3 stimulation alone supports poor T cell expansion, consistent with previous findings, 4-1BB was able to substitute for CD28 in the expansion of these T cells (Fig. S1 E). Functional profiling revealed these cells were potent effector T cells, and cells from combinatorial costimulation of CD28 and 4-1BB bore high expression of IL-2 and granzyme B (Fig. S1, F and G). Because 4-1BB signaling has been linked to metabolic reprogramming previously (Willoughby et al., 2014; Long et al., 2015; Choi et al., 2017), we asked how 4-1BB signaling modifies the metabolic profile of these previously activated, rested T cells. Flow cytometric analysis of these expanded cells showed 4-1BB-stimulated T cells have higher mitochondrial mass, as measured by MitoTracker FM staining (Fig. 1 A). Metabolic profiling using Seahorse analysis revealed that T cells stimulated and expanded for several days with 4-1BB have no appreciable differences in basal oxidative metabolism (Fig. 1 B, left) but rather harbor a dramatically increased respiratory capacity (Fig. 1 B, right). Interestingly, cotreatment with CD28 and 4-1BB agonists showed no increase in respiratory capacity but had significant increases in basal oxygen consumption rate (OCR), suggesting that 4-1BB might promote increases in mitochondrial content, whereas CD28 may promote mitochondrial function, consistent with previous studies (Fig. 1 B; Buck et al., 2016; Kawalekar et al., 2016). We also sought to determine the bioenergetic effects of this respiratory capacity. ATP levels in cells are relatively stable in nonstress situations, but ADP/ATP ratios can reveal a degree of metabolic readiness. We found that cells treated with 4-1BB (which have substantial respiratory capacity) have much higher intracellular levels of ADP compared with CD28 or cotreated cells, suggesting that these cells contain mitochondria energetically primed to produce ATP swiftly upon demand (Fig. 1 C).

4-1BB agonism has been considered an attractive strategy for the immunotherapy of cancer, providing an additional costimulatory signal within the tumor microenvironment. Thus, we wanted to also determine how 4-1BB agonism might affect T cell metabolism *in vivo*, even in the absence of tumor. We also wished to compare this therapy to PD-1 blockade, which has been previously associated with improving peripheral oxidative metabolism (Chamoto et al., 2017) and functions, in part, by enhancing CD28 signaling (Hui et al., 2017; Kamphorst et al., 2017), consistent with our manipulations *in vitro*. Indeed, PD-1 blockade resulted in a modest increase in oxidative metabolism of CD8⁺ T cells isolated from the peripheral lymph nodes of mice (Fig. 1, D and E). However, 4-1BB agonism, consistent with our *in vitro* findings, resulted in a striking increase in respiratory capacity of these cells (Fig. 1, D and E). 4-1BB also induced increases in basal T cell glycolysis, as measured by the extracellular acidification rate (ECAR; Fig. S2 A), but did not dramatically change the OCR/ECAR ratio (Fig. S2 B). Cotreatment with anti-PD-1 and anti-4-1BB resulted in significant increases in basal oxygen consumption (Fig. 1 E), suggesting that, from what we had observed *in vitro*, 4-1BB promotes increases in mitochondrial content, whereas PD-1 blockade-mediated costimulatory activity results

in increased oxidative function. We also confirmed that 4-1BB agonism *in vivo* improves ADP/ATP ratios, consistent with our *in vitro* energetic phenotyping of energetic priming of these cells (Fig. 1 F). We also profiled CD4⁺Foxp3⁻ and CD4⁺Foxp3⁺ T cells from Foxp3 reporter mice treated similarly. These analyses revealed that conventional and regulatory CD4⁺ T cells did not metabolically reprogram in response to 4-1BB agonist antibody treatment (Fig. S2, C and D). Thus, 4-1BB agonism, *in vitro* and *in vivo* can induce metabolic reprogramming, predominantly in oxidative metabolism, of CD8⁺ T cells.

We have previously shown that in tumor-infiltrating T cells, mitochondrial biogenesis is suppressed, in part because of inhibition of the transcriptional coactivator PGC1 α (Scharping et al., 2016). We reasoned that 4-1BB might support PGC1 α expression. Indeed, cells costimulated with 4-1BB show increased expression of PGC1 α (Fig. 1 G and Fig. S2 E). To determine the requirement for PGC1 α in this process, we repeated our studies in PGC1 α -deficient T cells from *Ppargc1a^{fl/fl}Cd4^{Cre}* mice. PGC1 α is required for 4-1BB-mediated increases in mitochondrial mass (Fig. 1 H) and respiratory capacity (Fig. 1, I and J). Thus, 4-1BB promotes metabolic reprogramming that involves PGC1 α -mediated pathways.

4-1BB costimulation results in increased mitochondrial fusion and biogenesis via p38-MAPK

We next wanted to determine the mechanism by which 4-1BB promotes increased mitochondrial content in T cells. To do this, we used short-term stimulation of T cells *in vitro* with 4-1BB agonist antibody. Even within 24 h of activation, 4-1BB was superior to CD28 at promoting increased respiratory capacity, similar to cells costimulated and expanded in the presence of 4-1BB ligation (Fig. 2 A). To identify whether there were any intracellular differences in mitochondrial volume or fusion, we conducted microscopic analysis of CD28- or 4-1BB-costimulated T cells retrovirally transduced with a construct encoding the mitochondrial protein TOM20 tagged to the enhanced GFP NeonGreen. Microscopic analysis of TOM20-NeonGreen-expressing T cells costimulated with anti-4-1BB revealed high mitochondrial volume and the presence of mitochondrial networking, suggesting increased mitochondrial fusion (Fig. 2 B). We also costained for mitofusin-2, which colocalized with mitochondria and had more intense, punctate staining in 4-1BB-treated cells (Fig. 2 B). Thus, we sought to determine how 4-1BB signaling might promote increased fusion and biogenesis. 4-1BB is a TNFR superfamily member and has been shown to activate p38-MAPK and NF- κ B (Munn, 2011), and in other cell types, p38-MAPK can activate the transcription factor ATF2 to promote mitochondrial fusion and biogenesis, in part through PGC1 α and mitofusins (Akimoto et al., 2005). Indeed, mitofusin-2 is a PGC1 α target gene, consistent with the hypothesis that mitochondrial biogenesis and fusion are linked (Bach et al., 2003). Signaling analyses of 4-1BB-costimulated T cells revealed activation of p38-MAPK, resulting in increases in activating phosphorylation of ATF2 and expression of mitofusin-2 (Fig. 2 C). PGC1 α , as a transcriptional coactivator, can bolster ATF2-mediated transcription of mitofusin-2. Indeed, 4-1BB stimulation promoted expression of mitofusin-2 in a manner that was diminished in the absence of PGC1 α (Fig. 2 D). We next wanted to identify whether p38 was

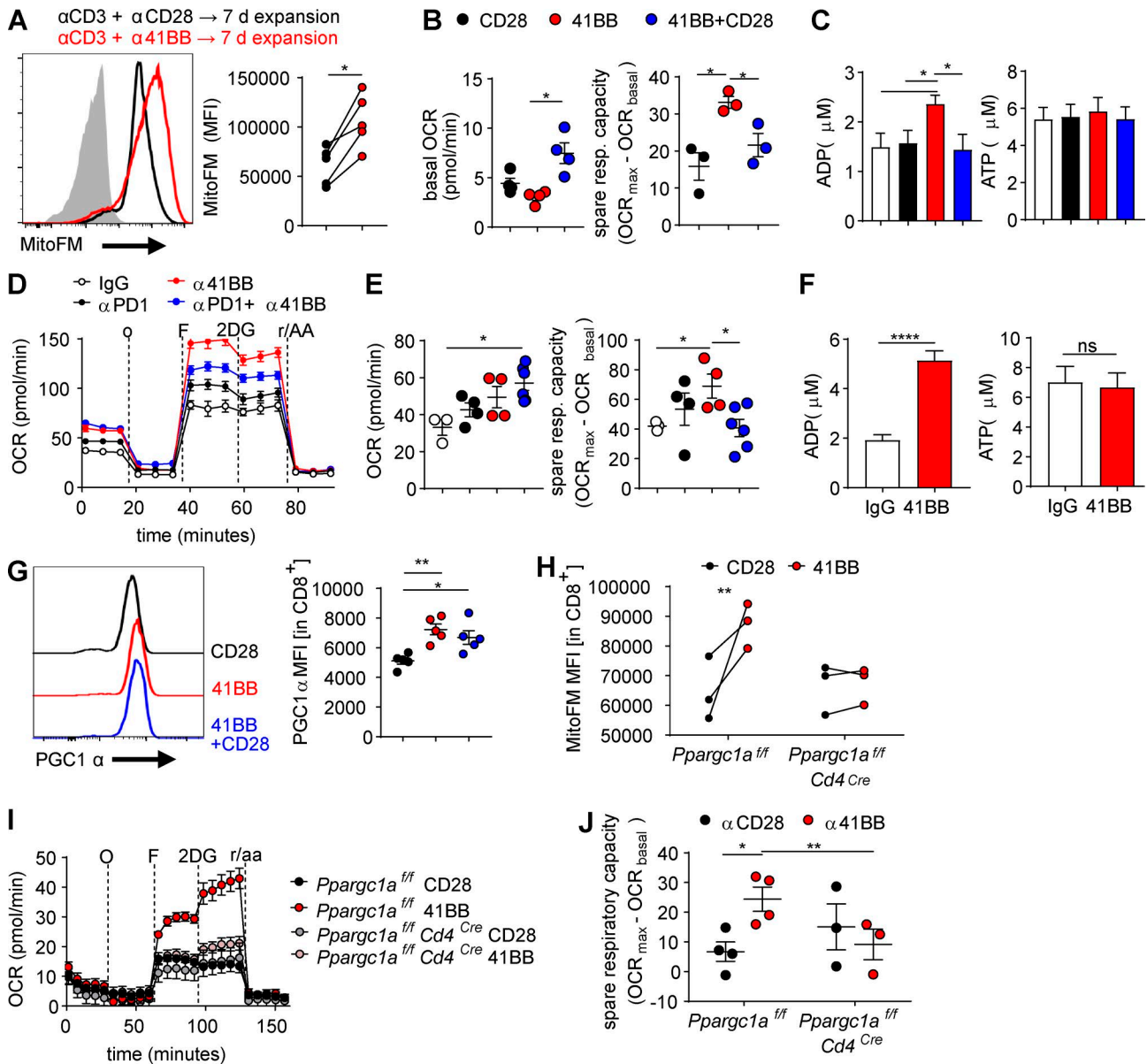


Figure 1. 4-1BB costimulation promotes PGC1 α -dependent mitochondrial function. (A) MitoTracker Deep Red FM staining of CD8⁺ T cells activated with immobilized anti-CD3 (3 μ g/ml plate-bound) in the presence of anti-CD28 (2 μ g/ml soluble), anti-4-1BB (10 μ g/ml soluble), or both for 24 h, then expanded with 25 U/ml IL-2 for 7 d. Shaded histogram indicates unstained control. (B) Baseline OCR and respiratory capacity of T cells expanded from CD28 or 4-1BB cultures. (C) Tabulated ATP and ADP concentrations from cells activated as in A but for 24 h. (D) Representative OCR trace of CD8⁺ T cells sorted from C57/BL6 mice treated with isotype control, anti-PD-1, anti-4-1BB, or both for 3 d. (E) Tabulated OCR (left) and spare respiratory capacity (right) T cells as in D. (F) Tabulated ATP and ADP concentrations from T cells as in D. (G) PGC1 α intracellular staining (left) of cells treated as in A. (H) MitoTracker Deep Red FM staining of cells from *Ppargc1a*^{fl/fl} or *Ppargc1a*^{fl/fl}*Cd4*^{Cre} mice treated as in A. (I and J) OCR trace (I) and respiratory capacity (J) of T cells from *Ppargc1a*^{fl/fl} or *Ppargc1a*^{fl/fl}*Cd4*^{Cre} mice treated as in A. Data represent three to five (A, C, and I) or represent the mean (B, D–H, and J) of three to five independent experiments. *, P < 0.05; **, P < 0.01; ***, P < 0.0001 by paired (A, B, H, and I) or unpaired (C–G) *t* test. Error bars indicate SEM.

the dominant signaling pathway for this effect. Costimulation in the presence of the p38-MAPK inhibitor SB202190 revealed that 4-1BB up-regulation of mitofusin (Fig. S2 F) and respiratory capacity (Fig. S2 G) was dependent on the activation of p38 signaling, returning to respiratory capacity of CD28 levels. SB202190 has been shown to have off-target effects (Shanware et al., 2009), so we also used retroviral-mediated RNA interference to the *Mapk14* gene encoding p38 α . Costimulation with 4-1BB failed to induce spare respiratory capacity or mitofusin-2 expression when cells were stably express shRNA targeting p38

(Fig. 2, E and F). Thus, 4-1BB signaling acts through p38-MAPK to promote increased mitochondrial respiratory capacity through PGC1 α and promote increased mitochondrial volume suggestive of mitochondrial fusion.

4-1BB agonists metabolically enable anti-PD-1 responses

To determine how 4-1BB-mediated changes in T cell metabolism might enable the immune response to cancer, we used B16 melanoma, an aggressive C57/BL6-derived cancer model that is insensitive to most standard immunotherapies. We found, consistent

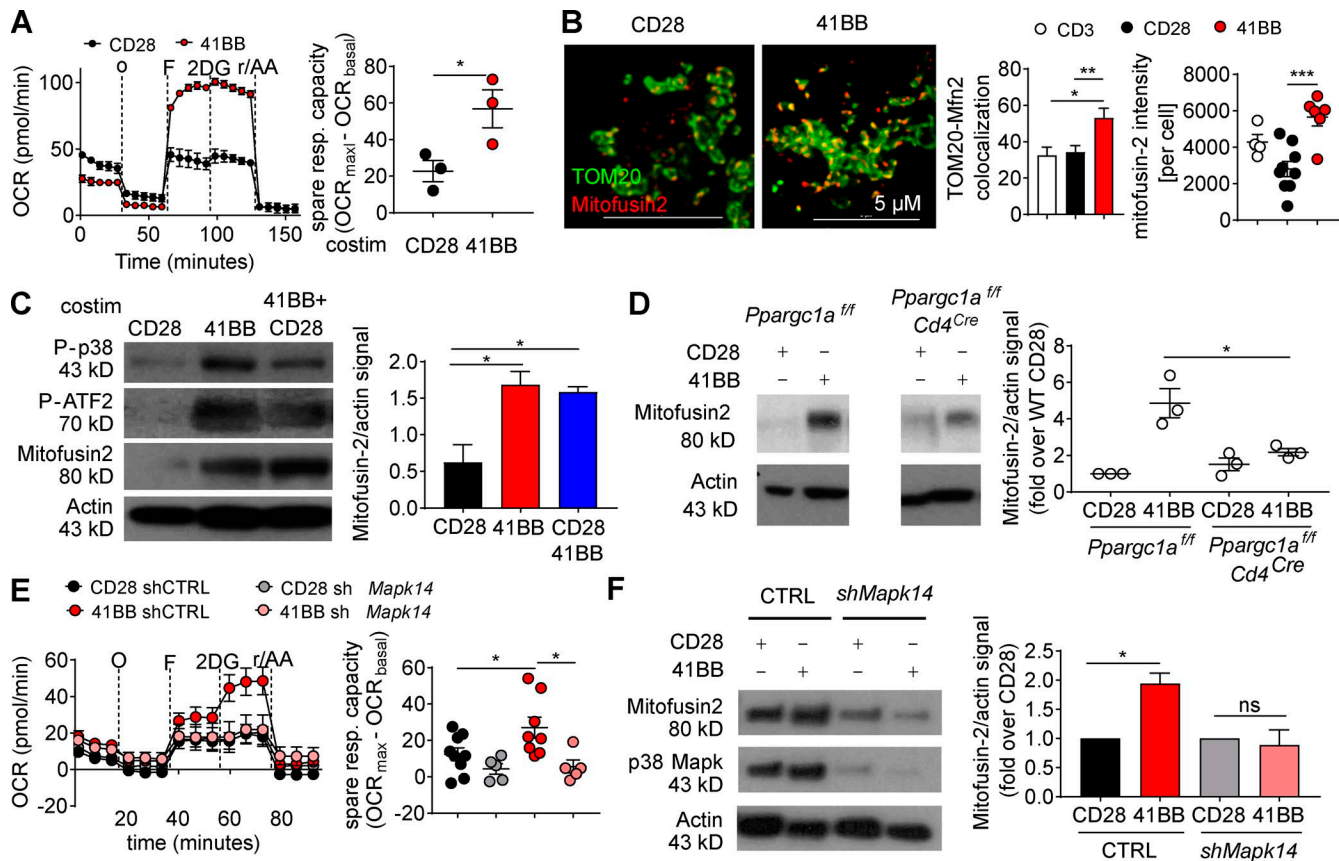


Figure 2. 4-1BB costimulation induces PGC1 α -dependent program of mitochondrial fusion and biogenesis through p38-MAPK. (A) Representative OCR trace and tabulated spare respiratory capacity of CD8⁺ T cells activated with 3 μ g/ml immobilized anti-CD3 in the presence of anti-CD28 (2 μ g/ml) or anti-4-1BB (10 μ g/ml) for 24 h. (B) Confocal imaging of mitochondria by using TOM20-NeonGreen-overexpressing T cells costimulated with CD28 or 4-1BB for 72 h. Tabulated data from multiple experiments are to the right. (C) Immunoblot (IB) analysis of cells activated as in A for 72 h. Densitometry from multiple experiments is tabulated to the right. (D) IB of mitofusin-2 in T cells from *Pparg1a*^{fl/fl} or *Pparg1a*^{fl/fl}*Cd4*^{Cre} mice stimulated in the presence of CD28 or 4-1BB agonistic antibodies for 72 h. Densitometry scanning from multiple experiments is tabulated to the right. (E) Representative OCR trace and tabulated SRC of CD8⁺ T cells retrovirally expressing scrambled control shRNA (shCTRL) or shRNA to *Mapk14* (encoding p38-MAPK) activated as in A and expanded in 25 U/ml IL-2 for 5 d. (F) IB analysis of mitofusin-2 in T cells activated as in E. Densitometry from multiple experiments is tabulated to the right. Data are representative of three (A, C, and D) or two (B, E, and F) independent experiments. *, P < 0.05; **, P < 0.01; ***, P < 0.001 by unpaired (A and F) or paired (D and F) *t* test. Error bars indicate SEM.

with a previous study in B16 melanoma (Chen et al., 2015), that PD-1 immunotherapy was ineffective in inducing antitumor responses and that 4-1BB monotherapy could slow tumor progression but fail to induce complete tumor regression (Fig. 3 A). However, the combination of these two therapies resulted in robust antitumor response (Fig. 3 A). We next characterized the metabolic makeup of the tumor infiltrate. We have previously shown that tumor-infiltrating T cells show decreased mitochondrial function and mass, mediated by repressed expression of PGC1 α (Scharping et al., 2016). We interrogated T cells from small B16 tumors treated for 3 d with these various therapies. Neither control treatment nor PD-1 therapy induced expression of PGC1 α in tumor-infiltrating lymphocytes (TILs), but with both anti-4-1BB and combination therapy we observed an increase in PGC1 α expression (Fig. 3 B). This was correlated with an increase in p38-MAPK activation (phosphorylation as measured by flow cytometry), suggesting 4-1BB was activating the p38 cascade in CD8⁺ TILs. (Fig. 3 C). 4-1BB or cotreatment prevented the loss of metabolic sufficiency typically observed in CD8⁺ TILs, as measured by

2NBDG uptake and MitoTracker FM staining (Fig. 3 D). Consistent with our agonist antibody treatment in non-tumor-bearing mice, CD4⁺ tumor-infiltrating T cells did not appear to be metabolically reprogrammed by 4-1BB agonism (Fig. S3). Thus, our data suggest that 4-1BB acts, at least in part, to improve the metabolic sufficiency of intratumoral T cells. We hypothesized that this heightened metabolic state primes these tumor-infiltrating T cells for activation, enabling their activity when PD-1-mediated inhibition of T cell activation is relieved.

4-1BB agonists enable adoptive cell therapy through PGC1 α

We next wanted to determine whether PGC1 α -mediated metabolic reprogramming was required for the immunostimulatory effects of 4-1BB in immunotherapy, using transfer of preactivated OT-I T cells into mice bearing OVA-expressing B16 melanoma as a model. Transfer of activated OT-I T cells into mice bearing small B16^{OVA} tumors results in a transient and incomplete tumor regression that can be markedly improved by treating recipient mice with 4-1BB agonist antibody (Fig. 4 A). However, this

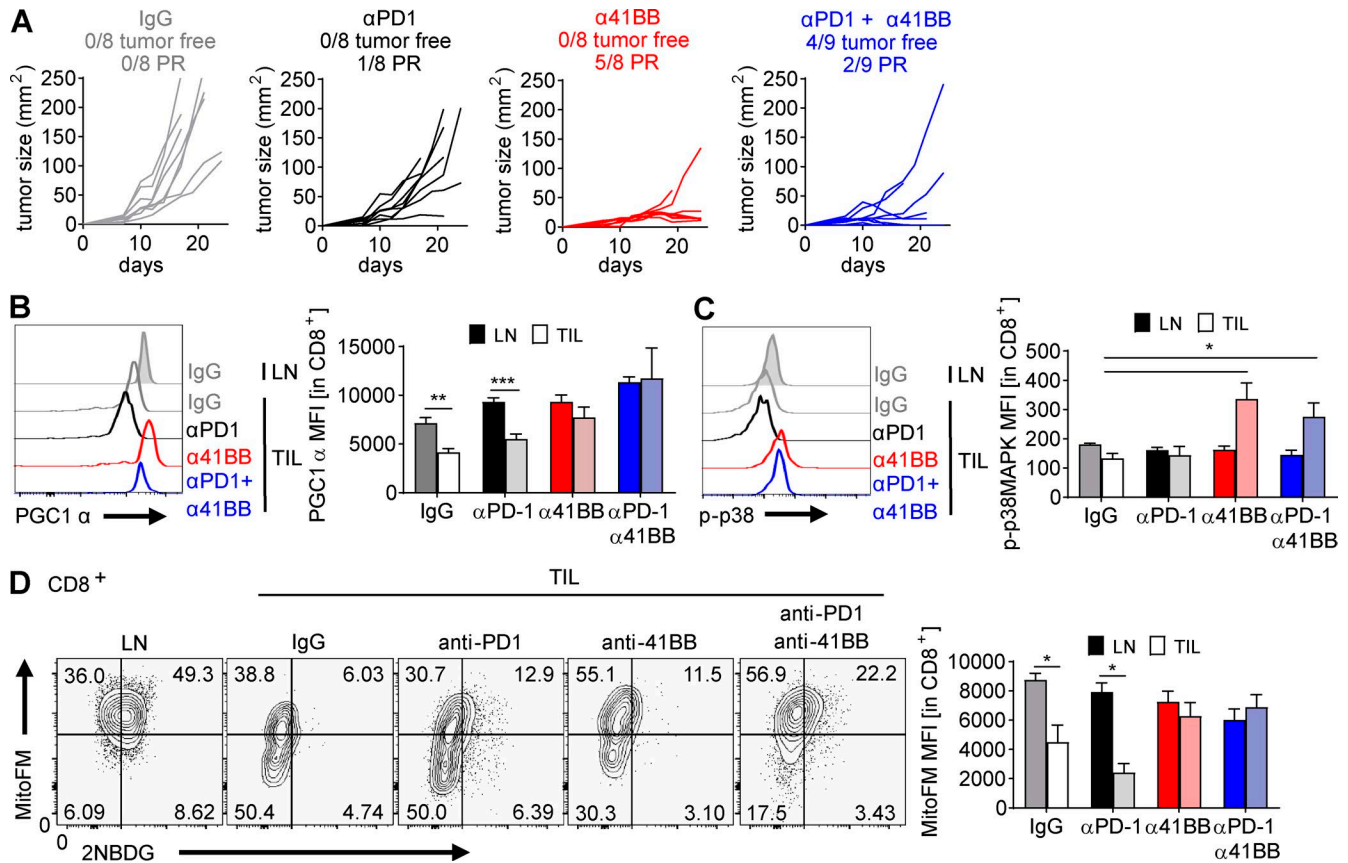


Figure 3. 4-1BB agonist antibodies metabolically support anti-PD-1 therapy. (A) Tumor growth curves of C57/BL6 mice inoculated with 100,000 B16-F10 melanoma cells intradermally. Mice received immunotherapy (200 μg anti-PD-1, 50 μg anti-4-1BB, or respective isotype controls three times weekly) when palpable tumors were detected (typically day 6–7). Each line represents one mouse. Tumor-free indicates a complete regression. PR indicates mice that did not completely regress but showed tumor regression for at least two measurements. **(B)** PGC1α staining (left) and tabulated data (right) from B16-bearing mice treated as indicated. LN, lymph node. **(C)** Phospho-p38 intracellular staining from B16-bearing mice treated as indicated. **(D)** Flow cytograms and tabulated data of glucose uptake (2NBDG) and mitochondrial staining (MitoFM) of CD8⁺ T cells from LNs or TILs of mice treated as in B. Data are representative of three independent experiments. *, $P < 0.05$; **, $P < 0.01$; ***, $P < 0.001$; by paired (B and D) or unpaired (C) *t* tests, or two-way ANOVA (A).

response was completely lost when the transferred OT-I T cells lacked PGC1α (Fig. 4 A). Although these data suggested 4-1BB's effects were solely on the transferred T cells, in this treatment strategy 4-1BB could still be acting on other cells in the micro-environment. Thus, we altered our strategy and limited 4-1BB treatment to the *in vitro* activation of the therapeutic T cells. Although less potent than *in vivo* treatment, 4-1BB-costimulated OT-I cells were superior therapeutic T cells, providing the only statistically significant decrease in tumor growth in our assay (Fig. 4 B). Again, this effect required expression of PGC1α (Fig. 4 B). Thus, our data suggest that 4-1BB agonism supports, in a PGC1α-dependent manner, increased T cell activity in adoptive cell therapy of cancer.

Our treatment strategy using 4-1BB-augmented T cells suggested that the metabolic support afforded by 4-1BB treatment appeared to persist, at least for days/weeks. Because clinical trials using 4-1BB agonism in patients have revealed dose-limiting toxicities associated with long-term treatment (Bartkowiak and Curran, 2015), we wondered whether 4-1BB synergy with PD-1-blockade therapy required continuous treatment or whether T cells could be metabolically reprogrammed before initiation of checkpoint blockade immunotherapy. To specifically test this,

we compared combination immunotherapy with a sequenced approach, in which 4-1BB was given for 3 d (sufficient to induce mitochondrial reprogramming; Fig. 3 D), followed by PD-1 blockade delivered in the absence of 4-1BB agonism. Mice receiving 4-1BB pretreatment showed the same synergistic response as 4-1BB cotreatment (Fig. 4 C), suggesting that metabolic support provided by 4-1BB agonism can be sequenced before initiation of checkpoint blockade immunotherapy to provide similar benefits, potentially without the risk of 4-1BB-mediated toxicities.

Concluding remarks

Our studies highlight the importance of metabolic sufficiency in the initiation and maintenance of antitumor immunity. Activation in the tumor, especially in a manner and environment that has no appreciable 4-1BB signaling, in combination with a nutrient-poor environment results in an unsustainable metabolic phenotype (Delgoffe and Powell, 2015). We have shown, both *in vivo* and *in vitro*, that 4-1BB stimulation results in up-regulation of PGC1α, which enhances mitochondrial networking and biogenesis, suggesting a phenotype of mitochondrial fusion. This is apparent metabolically through increases in respiratory capacity and energetically in steady-state elevation

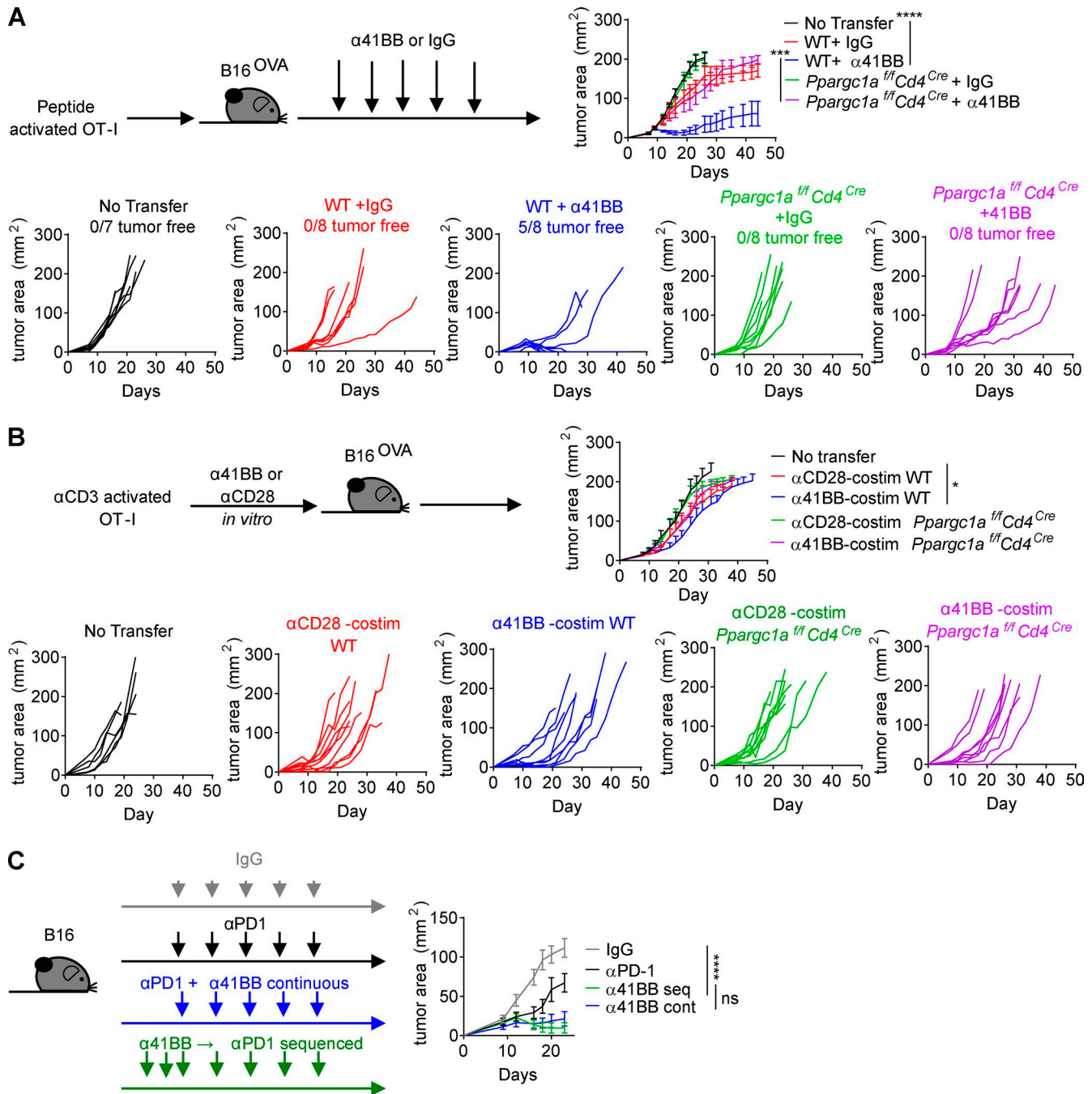


Figure 4. 4-1BB agonism improves adoptive T cell therapy through PGC1 α . (A) Tumor growth curves of C57/BL6 mice inoculated with 250,000 B16-OVA melanoma cells intradermally. Mice received an adoptive transfer of 2×10^6 CD8⁺ T cells from either WT OT-I or *Ppargc1a*^{fl/fl}*Cd4*^{Cre} OT-I mice. Mice then received immunotherapy, either 50 μ g anti-4-1BB or isotype control three times weekly. (B) Tumor growth curves of C57/BL6 mice inoculated with 250,000 B16-OVA melanoma cells intradermally. Mice received an adoptive transfer of 5×10^6 CD8⁺ T cells from either WT OT-I or *Ppargc1a*^{fl/fl}*Cd4*^{Cre} OT-I that were activated with immobilized anti-CD3 (3 μ g/ml plate-bound) in the presence of anti-CD28 (2 μ g/ml soluble) or anti-4-1BB (10 μ g/ml soluble) for 24 h and then expanded with 50 U/ml IL-2 for 7 d. (C) Tumor growth curves of C57/BL6 mice inoculated with 100,000 B16-F10 melanoma cells intradermally. Mice received immunotherapy (200 μ g anti-PD-1, 50 μ g anti-4-1BB, or respective isotype controls thrice weekly or anti-4-1BB for 3 d and then anti-PD-1 three times weekly) when palpable tumors were detected (typically day 5–6). Each line represents one animal. Tumor-free indicates a complete regression. Mean growth figures represent the mean of (A and C) or are representative of (B) two independent experiments. *, $P < 0.05$; ***, $P < 0.001$; ****, $P < 0.001$ by two-way ANOVA.

of ADP, indicative of metabolic “priming,” with mitochondria prepared to meet heightened ATP demands during activation. Our data support a critical role for costimulation in mitochondrial reprogramming, recently highlighted by a study of mitochondrial morphology in CD28 costimulation (Klein Geltink et al.,

2017). Our data comparing CD28 and 4-1BB suggest that 4-1BB stimulation may act to improve mitochondrial quality and capacity, whereas CD28 supports increased mitochondrial function and prepares the cell for the demands of differentiation and effector function.

Further, we have delineated the signaling pathways important for 4-1BB activity: specifically, activation of the p38-MAPK cascade promotes ATF2 activity, increasing PGC1 α levels as well as the levels of its target proteins, including mitofusin-2. This is largely in agreement with previously published work in non-immune cells, suggesting p38-MAPK regulates mitochondrial biogenesis (Bernard et al., 2015; Ihsan et al., 2015; Zhang et al., 2017). Because memory T cells are characterized by increased mitochondrial function (Pearce et al., 2013), we hypothesize that 4-1BB-elicited mitochondrial function fosters longevity, promoting a memory-like state, thought to be key in sustaining the antitumor immune response. Importantly, elevated “respiratory capacity” of mitochondria is routinely associated with longevity and, especially in T cells, supports an idea of metabolic priming. However, the physiological and functional importance of increased respiratory capacity has not been fully elucidated, especially in T cells, and may not simply be energetic. Thus, the importance of respiratory capacity certainly remains a subject for much future study.

Our data in models of cancer immunotherapy support the notion that 4-1BB signaling can provide metabolic support to T cells, consistent with previous studies both using chimeric antigen-receptor T cells with 4-1BB-signaling components (Long et al., 2015; Kawalekar et al., 2016) and basic studies using anti-4-1BB in vitro (Choi et al., 2017). This metabolic support, characterized most prominently by elevated mitochondrial sufficiency, enables immunotherapeutic responses, which, because of increases in T cell activation, require increased oxidative activity for their function. Our data using T cell-specific deletion of PGC1 α strongly suggest that metabolic reprogramming is the dominant function of 4-1BB costimulation, at least in the context of cancer immunology. Our work also strongly suggests that bolstering of T cell metabolism, through 4-1BB stimulation or other means, has the potential to improve antitumor immunity in cancer patients that may not respond to PD-1 therapy alone. Our sequencing study suggested that this metabolic support need not be continuous with PD-1 blockade, potentially mitigating any dose-limiting toxicities associated with 4-1BB agonism. These data are in agreement with recently published work using agonism of OX40, another TNFR superfamily member, which could be sequenced before PD-1 therapy for optimal effect (Messenheimer et al., 2017). We hypothesize that the TNFR family of costimulatory molecules may share metabolic reprogramming capacity; however, our data suggest these receptors may be expressed at different points during T cell differentiation from early activation through functional exhaustion. Future studies will determine how metabolic reprogramming can be used in combination with immunostimulatory therapies to provide increased responses in the immunotherapy of cancer.

Materials and methods

Mice

Animal work in this study was approved by the University of Pittsburgh Institutional Animal Care and Use Committee, accredited by the Association for Assessment and Accreditation of Laboratory Animal Care. Procedures were performed

under their guidelines. C57/BL6 mice were obtained originally from the Jackson Laboratories and bred in-house. *Ppargc1a^{fl/fl}*, *Cd4^{Cre}*, *Foxp3^{YFP-ICre}*, and OT-I mice were also obtained from Jackson Laboratories.

Cell culture

CD8⁺ T cells were isolated as previously described by using magnetic bead (MojoBeads; Biologend) negative isolation (Scharping et al., 2016). In expansion assays, T cells were activated 24 h with anti-CD3 (2C11, 3 μ g/ml) immobilized on tissue culture plates in the presence of anti-CD28 (37.51, 2 μ g/ml) or anti-4-1BB (3H3, 10 μ g/ml). After 24 h, cells were expanded 10-fold into fresh culture media in the presence of 50 U/ml murine IL-2 (PeproTech) and additional soluble costimulatory antibody. After 7 d of expansion, cells were counted and assayed. Cytokine production was measured by restimulating cells with immobilized anti-CD3 plus anti-CD28 for 18 h in vitro, with the final 5 h in the presence of a protein transport inhibitor.

Metabolic assays

T cell metabolic output was measured by Seahorse technology as previously described (Scharping et al., 2017). In brief, 100,000 T cells were seeded into Cell-Tak-coated XFe96 plates in minimal unbuffered assay media containing glucose and glutamine. Cells received sequential injections of 2 μ M oligomycin, 2 μ M FCCP, 10 mM 2-deoxyglucose, and 0.5 μ M rotenone/antimycin A.

For flow cytometric assays, cells were pulsed with 50 μ M 2-NBD-glucose (Cayman Chemical) in vitro for 30 min at 37°C. Cells were then surface stained at 4°C in the presence of 20 nM MitoTracker Deep Red FM for 15 min and then washed and assayed by flow cytometry. PGC1 α was measured by using anti-PGC1 α (H-300; Santa Cruz Biotechnology), anti-rabbit Alexa Fluor 647 (Jackson ImmunoResearch), and the Foxp3 Fix/Perm kit (eBioscience). Mitochondria were imaged by retrovirally transducing CD28- or 4-1BB-costimulated T cells with a Neon-Green-tagged TOM20 mitochondrial-imaging construct as previously described (Scharping et al., 2016). Mitofusin-2 imaging was performed on fixed and permeabilized samples by using an anti-mitofusin-2 antibody (Cell Signaling Technologies) and secondary antibody anti-rabbit linked to Alexa Fluor 555 (Life Technologies). Imaris Image Analysis and NIS-Elements Imaging Software were used to analyze imaging.

For ATP and ADP determination, CD8⁺ T cells were analyzed from C57/BL6 mice activated with anti-CD3 (2C11, 3 μ g/ml) immobilized on tissue culture plates in the presence of anti-CD28 (37.51, 2 μ g/ml), anti-4-1BB (3H3, 10 μ g/ml), or both or from cells isolated from C57/BL6 mice treated with 50 μ g anti-4-1BB (clone 3H3; Bio X-Cell) or respective rat isotype control, intraperitoneally every other day for 3 d. ATP and ADP concentrations were measured by using the ATP Determination kit (from Life Technologies) and the ADP Assay kit (from Sigma-Aldrich) according to the manufacturer’s instructions.

Immunoblot analysis

Cells were lysed in 1% NP-40 lysis buffer as previously described (Delgoffe et al., 2013). Lysates were separated by SDS-PAGE on 4–12% Bolt or Bio-Rad gels, transferred to polyvinylidene

difluoride membranes, and blocked in 3% BSA in Tris-buffered saline with 0.1% Tween-20. Primary antibodies to phospho-p38-MAPK, phospho-ATF2, Mitofusin-2, and actin (Cell Signaling Technologies) were added in 3% BSA/TBST for 1–2 h at room temperature or overnight at 4°C. Secondary antibodies (anti-rabbit or anti-mouse linked to horseradish peroxidase; Jackson ImmunoResearch) were added in 3% BSA/TBST for 1–2 h at room temperature. Enhanced chemiluminescence was visualized by using Western Lightning (PerkinElmer).

Retroviral RNA interference

Retroviral particles were generated by using Plat-E cell-mediated transfection. Spleen and lymph node preparations from C57/BL6 mice were stimulated with anti-CD3 (2C11, 3 µg/ml) immobilized on tissue culture plates in the presence of anti-CD28 (37.51, 2 µg/ml) or anti-4-1BB (3H3, 10 µg/ml). After 24 h, cultures were spininduced at 2,200 rpm for 120 min with retroviral supernatant in the presence of 6 µg/ml polybrene. After 2 h, media were changed. Cultures were then expanded for 5 d in 25 U/ml IL-2 and sorted on the top 50% of GFP⁺ cells. shRNA knockdown for each experiment was confirmed by immunoblot.

Immunotherapy and tumor models

C57/BL6 mice were treated with 200 µg anti-PD-1 (clone J43; Bio X-Cell), 50 µg anti-4-1BB (clone 3H3; Bio X-Cell), or respective hamster or rat isotype controls, intraperitoneally every other day for 3 d (in non-tumor-bearing experiments) or every other day for the duration of the experiment (in tumor experiments). For tumor growth experiments, mice were injected intradermally with 100,000 B16-F10 melanoma cells. When tumors were between 1 and 3 mm in any direction (typically day 6–7), mice began receiving immunotherapy. For TIL analysis experiments, tumors were allowed to reach 5–7 mm in any direction before initiation of immunotherapy in order to obtain sufficient cell numbers. For adoptive cell therapy experiments, mice received B16^{OVA} intradermally. OT-I T cells were activated *in vitro* by using either SIINFEKL peptide (500 nM) or anti-CD3 stimulation in combination with anti-CD28 or anti-4-1BB, followed by an expansion in 50 U/ml recombinant mouse IL-2. When tumors were between 1 and 3 mm in any direction (typically day 7–8), mice received an intravenous adoptive transfer of 2 × 10⁶ or 5 × 10⁶ OT-I cells. In systemic immunotherapy experiments, mice then began receiving 50 µg anti-4-1BB or its isotype control intraperitoneally.

Online supplemental material

Fig. S1 shows 4-1BB (CD137) was highly up-regulated on terminally exhausted T cells, whereas molecules such as CD28, ICOS, and OX40 are repressed or unchanged, and 4-1BB costimulation was able to substitute for CD28 by supporting the expansion and function of murine CD8⁺ T cells. Fig. S2 shows CD4⁺ T cells and regulatory T cells do not metabolically reprogram with 4-1BB agonist antibody treatment. Also, 4-1BB-mediated metabolic reprogramming is signaling through p38-MAPK. Fig. S3 shows CD4⁺ tumor-infiltrating T cells are not metabolically reprogrammed by 4-1BB agonism.

Menk et al.

4-1BB metabolically supports T cell function

Acknowledgments

This work was supported by the Sidney Kimmel Foundation for Cancer Research (SKF-015-036), Stand Up To Cancer–American Association for Cancer Research (SU2C-AACR-IRG-04-16), a National Institutes of Health Director's New Innovator Award (DP2AI136598), and the Cancer Institute, University of Pittsburgh Melanoma and Head and Neck Cancer SPOREs (to G.M. Delgoffe), and T32 CA082084 and F99CA222711 (to N.E. Scharping). This work utilized the UPMC Hillman Cancer Center Flow Cytometry and Animal Facilities, supported in part by P30CA047904.

The authors declare no competing financial interests.

Author contributions: A.V. Menk conducted the majority of the research, analyzed data, and helped write the manuscript. N.E. Scharping performed crucial initial experiments and conducted adoptive transfer experiments. D.B. Rivadeneira prepared and analyzed microscopy and conducted immunotherapy experiments. M.J. Calderon generated microscopic data. M.J. Watson conducted RNAi experiments. D. Dunstane assisted with mouse experiments. S.C. Watkins provided microscopic analysis support. G.M. Delgoffe conceived of and oversaw research, performed several experiments, analyzed data, obtained research funding, and wrote the manuscript.

Submitted: 13 June 2017

Revised: 18 December 2017

Accepted: 8 February 2018

References

- Akimoto, T., S.C. Pohnert, P. Li, M. Zhang, C. Gumbs, P.B. Rosenberg, R.S. Williams, and Z. Yan. 2005. Exercise stimulates Pgc-1α transcription in skeletal muscle through activation of the p38 MAPK pathway. *J. Biol. Chem.* 280:19587–19593. <https://doi.org/10.1074/jbc.M408862200>
- Bach, D., S. Pich, F.X. Soriano, N. Vega, B. Baumgartner, J. Oriola, J.R. Daugaard, J. Lloberas, M. Camps, J.R. Zierath, et al. 2003. Mitofusin-2 determines mitochondrial network architecture and mitochondrial metabolism. A novel regulatory mechanism altered in obesity. *J. Biol. Chem.* 278:17190–17197. <https://doi.org/10.1074/jbc.M212754200>
- Bartkowiak, T., and M.A. Curran. 2015. 4-1BB agonists: Multi-potent potentiators of tumor immunity. *Front. Oncol.* 5:117. <https://doi.org/10.3389/fonc.2015.00117>
- Bernard, K., N.J. Logsdon, S. Ravi, N. Xie, B.P. Persons, S. Rangarajan, J.W. Zmijewski, K. Mitra, G. Liu, V.M. Darley-Usmar, and V.J. Thannickal. 2015. Metabolic reprogramming is required for myofibroblast contractility and differentiation. *J. Biol. Chem.* 290:25427–25438. <https://doi.org/10.1074/jbc.M115.646984>
- Buck, M.D., D. O'Sullivan, R.I. Klein Geltink, J.D. Curtis, C.H. Chang, D.E. Sanin, J. Qiu, O. Kretz, D. Braas, G.J. van der Windt, et al. 2016. Mitochondrial dynamics controls T cell fate through metabolic programming. *Cell.* 166:63–76. <https://doi.org/10.1016/j.cell.2016.05.035>
- Callahan, M.K., M.A. Postow, and J.D. Wolchok. 2016. Targeting T cell co-receptors for cancer therapy. *Immunity.* 44:1069–1078. <https://doi.org/10.1016/j.immuni.2016.04.023>
- Chamoto, K., P.S. Chowdhury, A. Kumar, K. Sonomura, F. Matsuda, S. Fagarsan, and T. Honjo. 2017. Mitochondrial activation chemicals synergize with surface receptor PD-1 blockade for T cell-dependent antitumor activity. *Proc. Natl. Acad. Sci. USA.* 114:E761–E770. <https://doi.org/10.1073/pnas.1620433114>
- Chang, C.H., J.D. Curtis, L.B. Maggi Jr., B. Faubert, A.V. Villarino, D. O'Sullivan, S.C. Huang, G.J. van der Windt, J. Blagih, J. Qiu, et al. 2013. Posttranscriptional control of T cell effector function by aerobic glycolysis. *Cell.* 153:1239–1251. <https://doi.org/10.1016/j.cell.2013.05.016>
- Chen, S., L.F. Lee, T.S. Fisher, B. Jessen, M. Elliott, W. Evering, K. Logronio, G.H. Tu, K. Tsaparikos, X. Li, et al. 2015. Combination of 4-1BB agonist and PD-1 antagonist promotes antitumor effector/memory CD8 T cells

- in a poorly immunogenic tumor model. *Cancer Immunol. Res.* 3:149–160. <https://doi.org/10.1158/2326-6066.CIR-14-0118>
- Choi, B.K., D.Y. Lee, D.G. Lee, Y.H. Kim, S.-H. Kim, H.S. Oh, C. Han, and B.S. Kwon. 2017. 4-1BB signaling activates glucose and fatty acid metabolism to enhance CD8⁺T cell proliferation. *Cell. Mol. Immunol.* 14:748–757. <https://doi.org/10.1038/cmi.2016.02>
- Delgoffe, G.M. 2016. Filling the tank: Keeping antitumor T cells metabolically fit for the long haul. *Cancer Immunol. Res.* 4:1001–1006. <https://doi.org/10.1158/2326-6066.CIR-16-0244>
- Delgoffe, G.M., and J.D. Powell. 2015. Feeding an army: The metabolism of T cells in activation, energy, and exhaustion. *Mol. Immunol.* 68(2, 2 Pt C):492–496. <https://doi.org/10.1016/j.molimm.2015.07.026>
- Delgoffe, G.M., S.R. Woo, M.E. Turnis, D.M. Gravano, C. Guy, A.E. Overacre, M.L. Bettini, P. Vogel, D. Finkelstein, J. Bonnevier, et al. 2013. Stability and function of regulatory T cells is maintained by a neuropilin-1-semaphorin-4a axis. *Nature.* 501:252–256. <https://doi.org/10.1038/nature12428>
- Fernandez-Marcos, P.J., and J. Auwerx. 2011. Regulation of PGC-1 α , a nodal regulator of mitochondrial biogenesis. *Am. J. Clin. Nutr.* 93:884S–890S. <https://doi.org/10.3945/ajcn.110.001917>
- Ferris, R.L., G. Blumenschein Jr., J. Fayette, J. Guigay, A.D. Colevas, L. Licitra, K. Harrington, S. Kasper, E.E. Vokes, C. Even, et al. 2016. Nivolumab for recurrent squamous-cell carcinoma of the head and neck. *N. Engl. J. Med.* 375:1856–1867. <https://doi.org/10.1056/NEJMoa1602252>
- Gubser, P.M., G.R. Bantug, L. Razik, M. Fischer, S. Dimeloe, G. Hoenger, B. Durovic, A. Jauch, and C. Hess. 2013. Rapid effector function of memory CD8⁺ T cells requires an immediate-early glycolytic switch. *Nat. Immunol.* 14:1064–1072. <https://doi.org/10.1038/ni.2687>
- Hui, E., J. Cheung, J. Zhu, X. Su, M.J. Taylor, H.A. Wallweber, D.K. Sasmal, J. Huang, J.M. Kim, I. Mellman, and R.D. Vale. 2017. T cell costimulatory receptor CD28 is a primary target for PD-1-mediated inhibition. *Science.* 355:1428–1433. <https://doi.org/10.1126/science.aaf1292>
- Ihsan, M., J.F. Markworth, G. Watson, H.C. Choo, A. Govus, T. Pham, A. Hickey, D. Cameron-Smith, and C.R. Abbiss. 2015. Regular postexercise cooling enhances mitochondrial biogenesis through AMPK and p38 MAPK in human skeletal muscle. *Am. J. Physiol. Regul. Integr. Comp. Physiol.* 309:R286–R294. <https://doi.org/10.1152/ajpregu.00031.2015>
- Jacobs, S.R., C.E. Herman, N.J. Maciver, J.A. Wofford, H.L. Wieman, J.J. Hammen, and J.C. Rathmell. 2008. Glucose uptake is limiting in T cell activation and requires CD28-mediated Akt-dependent and independent pathways. *J. Immunol.* 180:4476–4486. <https://doi.org/10.4049/jimmunol.180.7.4476>
- Kamphorst, A.O., A. Wieland, T. Nasti, S. Yang, R. Zhang, D.L. Barber, B.T. Konieczny, C.Z. Daugherty, L. Koenig, K. Yu, et al. 2017. Rescue of exhausted CD8 T cells by PD-1-targeted therapies is CD28-dependent. *Science.* 355:1423–1427. <https://doi.org/10.1126/science.aaf0683>
- Kawalekar, O.U., R.S. O'Connor, J.A. Fraietta, L. Guo, S.E. McGettigan, A.D. Posey Jr., P.R. Patel, S. Guedan, J. Scholler, B. Keith, et al. 2016. Distinct signaling of coreceptors regulates specific metabolism pathways and impacts memory development in CAR T cells. *Immunity.* 44:380–390. <https://doi.org/10.1016/j.immuni.2016.01.021>
- Klein Geltink, R.I., D. O'Sullivan, M. Corrado, A. Bremser, M.D. Buck, J.M. Buescher, E. Firat, X. Zhu, G. Niedermann, G. Caputa, et al. 2017. Mitochondrial Priming by CD28. *Cell.* 171:385–397.e11. <https://doi.org/10.1016/j.cell.2017.08.018>
- Long, A.H., W.M. Haso, J.F. Shern, K.M. Wanhainen, M. Murgai, M. Ingarano, J.P. Smith, A.J. Walker, M.E. Kohler, V.R. Venkateshwara, et al. 2015. 4-1BB costimulation ameliorates T cell exhaustion induced by tonic signaling of chimeric antigen receptors. *Nat. Med.* 21:581–590. <https://doi.org/10.1038/nm.3838>
- Messenheimer, D.J., S.M. Jensen, M.E. Afentoulis, K.W. Wegmann, Z. Feng, D.J. Friedman, M.J. Gough, W.J. Urba, and B.A. Fox. 2017. Timing of PD-1 blockade is critical to effective combination immunotherapy with anti-OX40. *Clin. Cancer Res.* 23:6165–6177. <https://doi.org/10.1158/1078-0432.CCR-16-2677>
- Munn, D.H. 2011. Indoleamine 2,3-dioxygenase, Tregs and cancer. *Curr. Med. Chem.* 18:2240–2246. <https://doi.org/10.2174/0929867117956656045>
- Pearce, E.L., M.C. Poffenberger, C.H. Chang, and R.G. Jones. 2013. Fueling immunity: insights into metabolism and lymphocyte function. *Science.* 342:1242454. <https://doi.org/10.1126/science.1242454>
- Peng, M., N. Yin, S. Chhangawala, K. Xu, C.S. Leslie, and M.O. Li. 2016. Aerobic glycolysis promotes T helper 1 cell differentiation through an epigenetic mechanism. *Science.* 354:481–484. <https://doi.org/10.1126/science.aaf6284>
- Rathmell, J.C., R.L. Elstrom, R.M. Cinalli, and C.B. Thompson. 2003. Activated Akt promotes increased resting T cell size, CD28-independent T cell growth, and development of autoimmunity and lymphoma. *Eur. J. Immunol.* 33:2223–2232. <https://doi.org/10.1002/eji.200324048>
- Sanchez-Paulete, A.R., S. Labiano, M.E. Rodriguez-Ruiz, A. Azpilikueta, I. Etxebarria, E. Bolaños, V. Lang, M. Rodriguez, M.A. Aznar, M. Jure-Kunkel, and I. Melero. 2016. Deciphering CD137 (4-1BB) signaling in T-cell costimulation for translation into successful cancer immunotherapy. *Eur. J. Immunol.* 46:513–522. <https://doi.org/10.1002/eji.201445388>
- Scharping, N.E., and G.M. Delgoffe. 2016. Tumor microenvironment metabolism: A new checkpoint for anti-tumor immunity. *Vaccines (Basel).* 4:46. <https://doi.org/10.3390/vaccines4040046>
- Scharping, N.E., A.V. Menk, R.S. Moreci, R.D. Whetstone, R.E. Dadey, S.C. Watkins, R.L. Ferris, and G.M. Delgoffe. 2016. The tumor microenvironment represses T cell mitochondrial biogenesis to drive intratumoral T cell metabolic insufficiency and dysfunction. *Immunity.* 45:374–388. <https://doi.org/10.1016/j.immuni.2016.07.009>
- Scharping, N.E., A.V. Menk, R.D. Whetstone, X. Zeng, and G.M. Delgoffe. 2017. Efficacy of PD-1 blockade is potentiated by metformin-induced reduction of tumor hypoxia. *Cancer Immunol. Res.* 5:9–16. <https://doi.org/10.1158/2326-6066.CIR-16-0103>
- Segal, N.H., T.F. Logan, F.S. Hodi, D. McDermott, I. Melero, O. Hamid, H. Schmidt, C. Robert, V. Chiarion-Sileni, P.A. Ascierto, et al. 2017. Results from an integrated safety analysis of urelumab, an agonist anti-CD137 monoclonal antibody. *Clin. Cancer Res.* 23:1929–1936. <https://doi.org/10.1158/1078-0432.CCR-16-1272>
- Shanware, N.P., L.M. Williams, M.J. Bowler, and R.S. Tibbetts. 2009. Non-specific in vivo inhibition of CK1 by the pyridinyl imidazole p38 inhibitors SB 203580 and SB 202190. *BMB Rep.* 42:142–147. <https://doi.org/10.5483/BMBRep.2009.42.3.142>
- van der Windt, G.J., D. O'Sullivan, B. Everts, S.C. Huang, M.D. Buck, J.D. Curtis, C.H. Chang, A.M. Smith, T. Ai, B. Faubert, et al. 2013. CD8 memory T cells have a bioenergetic advantage that underlies their rapid recall ability. *Proc. Natl. Acad. Sci. USA.* 110:14336–14341. <https://doi.org/10.1073/pnas.1221740110>
- Wherry, E.J., and M. Kurachi. 2015. Molecular and cellular insights into T cell exhaustion. *Nat. Rev. Immunol.* 15:486–499. <https://doi.org/10.1038/nri3862>
- Williams, J.B., B.L. Horton, Y. Zheng, Y. Duan, J.D. Powell, and T.F. Gajewski. 2017. The EGR2 targets LAG-3 and 4-1BB describe and regulate dysfunctional antigen-specific CD8⁺ T cells in the tumor microenvironment. *J. Exp. Med.* 214:381–400. <https://doi.org/10.1084/jem.20160485>
- Willoughby, J.E., J.P. Kerr, A. Rogel, V.Y. Taraban, S.L. Buchan, P.W. Johnson, and A. Al-Shamkhani. 2014. Differential impact of CD27 and 4-1BB costimulation on effector and memory CD8 T cell generation following peptide immunization. *J. Immunol.* 193:244–251. <https://doi.org/10.4049/jimmunol.1301217>
- Zang, X., and J.P. Allison. 2007. The B7 family and cancer therapy: costimulation and coinhibition. *Clin. Cancer Res.* 13:5271–5279. <https://doi.org/10.1158/1078-0432.CCR-07-1030>
- Zhang, T., T. Ikejima, L. Li, R. Wu, X. Yuan, J. Zhao, Y. Wang, and S. Peng. 2017. Impairment of Mitochondrial Biogenesis and Dynamics Involved in Isoniazid-Induced Apoptosis of HepG2 Cells Was Alleviated by p38 MAPK Pathway. *Front. Pharmacol.* 8:753. <https://doi.org/10.3389/fphar.2017.00753>
- Zheng, Y., G.M. Delgoffe, C.F. Meyer, W. Chan, and J.D. Powell. 2009. Anergic T cells are metabolically anergic. *J. Immunol.* 183:6095–6101. <https://doi.org/10.4049/jimmunol.0803510>